Desalination and Water Treatment
www.deswater.com
doi: 10.1080/19443994.2013.812988

52 (2014) 2009–2016
February

Taylor & Francis
Taylor & Francis Group

Geostatistical optimization of water reservoir characterization case of the "Jeffra de Medenine" aquifer system (SE Tunisia)

Hayet Chihi[a,*], Nicolas Jeannee[b], Houcine Yahyaoui[c], Habib Belayouni[d], Mourad Bedir[a]

[a]*Georesources Laboratory, Centre for Water Researches and Technologies, University of Carthage, Borj Cedria Ecopark, BP 273, Soliman, Tunisia*
Email: hayet_chihi@yahoo.fr
[b]*Geovariances, 49 bis Av Franklin Roosevelt, 77215 Avon Cedex, Paris, France*
[c]*Regional Commissary for Agricultural Development of Medenine, Medenine, Tunisia*
[d]*Faculty of Sciences of Tunis, Department of Geology, University Tunis El Manar, 1068 Tunis, Tunisia*

Received 25 December 2012; Accepted 24 May 2013

ABSTRACT

This study attempts to characterize the organization, geometry and continuity of aquifer systems in a faulted setting, by geostatistical methods. It concerns the "Jeffara de Medenine" aquifers, in South-Eastern Tunisia. The quality of architectural reservoir modelling depends heavily on available data and on the fault network at the origin of its compartmentalization. In our case study, the available data consist mainly of boreholes: (i) usually sparse: the data distribution and density are very uneven within the study area, depending on the aquifers and the river network; (ii) they do not, usually penetrate the entire aquifer formation. Therefore, aquifers situated at a great depth remain unattainable for many drillings, leaving large areas under-informed and (iii) they are supplemented by seismic data which, although of variable quality, provide useful information for building the fault network at a large scale. To deal with this lack of data, an original geostatistical approach is applied in order to make the best use of the available data: (i) borehole data corresponding to the geological interfaces: these are exact data (equal to) and (ii) information provided by the end of drilling; these are uncertain data using inequalities (less than, greater than, between). The estimation of the Turonian reservoir top (taken as an example in this study) may indeed be constrained by the exact and inequality well values, thus avoiding some inconsistencies during interpolation by kriging under inequality constraints. Fault parameters are also explicitly incorporated in the interpolation procedure. This geostatistical approach is used for depth estimation within the "Jeffara de Medenine" aquifer system and is compared to classical kriging and evaluated through the quality of estimation, the adopted assumptions and method limitations. Thus, estimation procedures can be improved to build geometric models that describe as well as possible the geological reality.

*Corresponding author.

Presented at the 6th International Conference on Water Resources in Mediterranean Basin (WATMED6), 10–12 October 2012, Sousse, Tunisia

Keywords: Architectural Model; Geostatistics; Kriging with inequality; Aquifer system; Borehole; Sparse data; Faults

1. Introduction

In southern Tunisia, good-quality water resources are relatively rare and are not easily renewed due to the semi-arid climate in this area. The lack of resources is the result mainly of the significant demographic growth, which has caused an increase in the demand for water both for irrigation and for drinking. In addition, the area now faces a serious problem of water-quality deterioration caused by considerable economic growth coupled with overexploitation of water resources.

The aquifers supply the area with water of a salinity varying from 1 to 7 g/l. The reasons for this relatively high mineralization are marine intrusion, brackish water intrusions drained from adjacent salty systems and the proximity of hyper-saline water systems like Sebkhas and Chotts.

The study area (Fig. 1), the "Jeffara de Medenine", includes a multi-aquifer system called the Zeuss Koutine aquifer which is the main water resource in the area. It is a vulnerable system and hence needs to be further documented and monitored in order to preserve it and improve its water quality.

One of the most important features that characterize this water system is its geological complexity, in particular due to the intense tectonics affecting the various aquifers. In general, fault systems influence communication between reservoirs. For a better understanding of the water flow paths within the faulted reservoir units, it is imperative to build the reservoir architecture of the site where the geometry of the units and their spatial extensions are established.

Geometric modelling of each water reservoir unit implies that the spatial distribution of the depth variable within each surface boundary is estimated. However, high spatial variability of "depth" within a faulted surface boundary and sparse data network are known to be major causes of uncertainty.

Our major goal in this study is to investigate whether geostatistical techniques can accurately reconstruct the unknown surfaces on the basis of values observed at a small number of points in the study area. Classical kriging was first applied, to account for the spatial continuity of the target horizons through the variogram analysis. Kriging also allows explicit integration of the fault system knowledge in the estimation process. Then, an original kriging variant, called kriging with inequality constraints was tested to avoid losing the information from wells which had not reached the target horizon. Although not new, to our knowledge, this methodology has not been applied previously to the modelling of aquifers.

2. Materials and methods

The construction of a geologically consistent reservoir model involved the following major steps: (i)

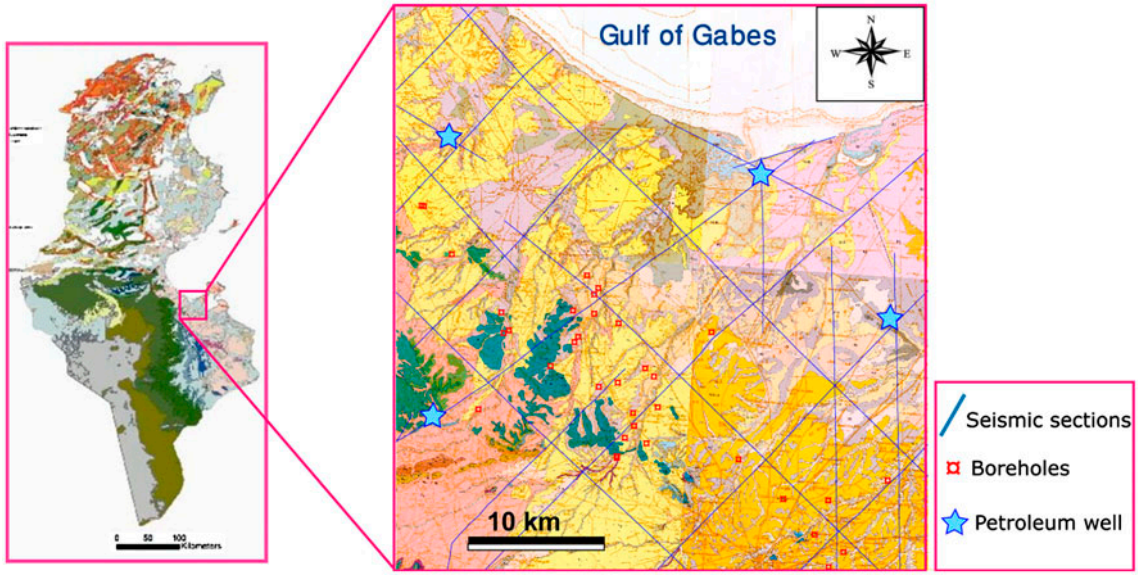

Fig. 1. Map of the studied domain and data location.

creation of a structural framework, (ii) delineation of the reservoir and (iii) integration of different types of information through geostatistical techniques to model the surfaces bounding the reservoir units using the ISATIS software [1].

2.1. Data base

Data and information were obtained from different sources and studies [2–6]: 16 seismic cross-sections, four petroleum wells as well as 49 water wells and boreholes (Fig. 1) were used to provide direct information on the surface and subsurface geology needed for the spatial modelling of the different bounding surfaces.

Each data type has its specific features, which influence how it is integrated into the modelling process and affect the quality of the model. However, these raw data alone would be useless without careful and methodical processing and interpretation. Georeferencing is a crucial step in the modelling process, whereby all available information is combined and organized in a common coordinate system: it has to cover the entire studied zone and to be precise enough not to lose or distort information.

2.2. Geologic exploration: building a structural framework

The proposed modelling methodology starts with a careful geological analysis of (i) the lithostratigraphic units that compose the aquifer system within the study area and (ii) fault structures that affect the different reservoir units. The objective is to improve the reservoir characterization of the aquifer system in order to define the geometric parameters required for the geometric modelling steps.

The multi-aquifer system includes all the layers from the Jurassic to the Mio-plio-quaternary. The carbonate formations of the Jurassic, the Albo-Aptian, the Turonian and the lower Senonian constitute a multilayer hydrogeological unit [3,4]. The lateral extent of the different aquifers at various depths is controlled by the structural evolution of the area and its vicinity during Jurassic to present times [2,4]. The connections between aquifers are possible either through faults or by vertical leakage.

Two main fault classes were identified: (i) the large-scale faults inferred from seismic data [5,6] and (ii) the small-scale faults observed on geological cross-sections reconstructed through lithostratigraphic correlation using boreholes (Fig. 2) or documented on geological maps [7].

Figs. 2 and 3 show the most prominent fault structures identified and correlated in the studied area, they display a NW-SE striking trend with throws towards the NE. These faults run from SW to NE: the Tebaga fault, the Medenine fault, the Mareth fault, the Zarat fault, the Lella Gamoudia fault and the Oum Zassar fault. Several minor, unevenly spaced faults in the studied field were mapped on the geologic cross-sections. The main ones were correlated and they are the Ksar Chrarif fault, the Zeuss fault and the Koutine fault. They display a NE-SW striking trend with throws towards the NW for the Ksar Chrarif and Koutine faults and to the SE for the Zeuss faults. All these faults created the compartmentalization of the area and built up a system of horst and graben structures, within a globally down-tilted domain towards the NE.

This fault classification has several important implications from a modelling point of view, as it allows a definition of the fault hierarchy that has to be included in the modelling procedures.

2.3. Geostatistical modelling

A consistent architectural model is constituted not only of the surfaces that fit the observation data, but also of correct relationships between the geological interfaces. For this purpose, classical kriging and kriging with inequality constraint estimates are compared and evaluated in order to build geometric models that reflect as well as possible the geological reality.

These kriging estimators are but variants of the basic linear regression estimator. They are based on the regionalized variable theory where the value of a variable $z(x)$ at a point with coordinates vector x is considered a realization of a random variable $Z(x)$. The collection of spatially correlated random variables $\{Z(x),\ x \in R\}$, where R denotes the study region, is termed a random function [8].

2.3.1. Ordinary kriging

We consider the problem of estimating the value of the target variable "depth", at any unsampled location x, of a bounding surface using a given neighbourhood $\{Z(X_\alpha)\alpha = 1, \ldots, n\}$, at the same bounding surface. The kriging estimator is a linear regression estimator $Z^*(x)$ defined as:

$$Z^*(x) = \sum_{\alpha=1}^{n} \lambda_\alpha Z(x_\alpha) \quad (1)$$

where λ_α is the weight assigned to $Z(x_\alpha)$ [9].

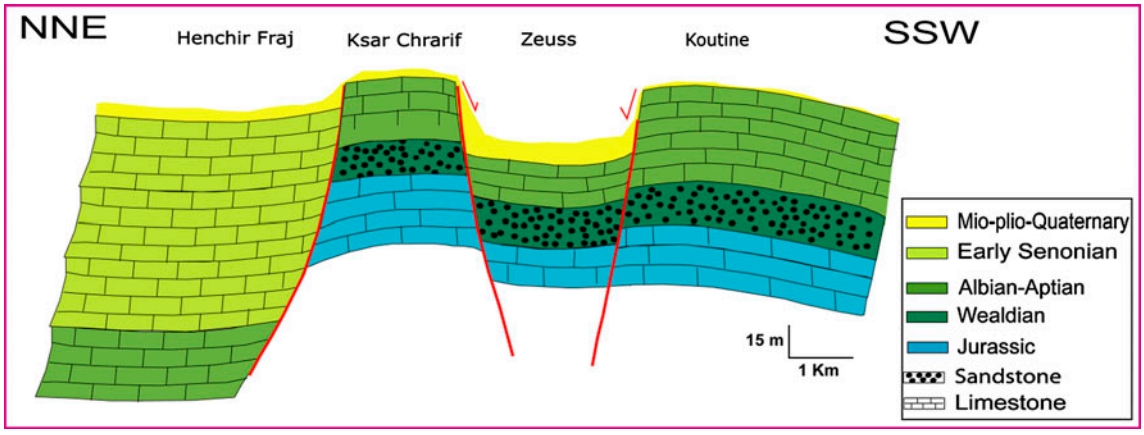

Fig. 2. Geologic cross-section within the study area.

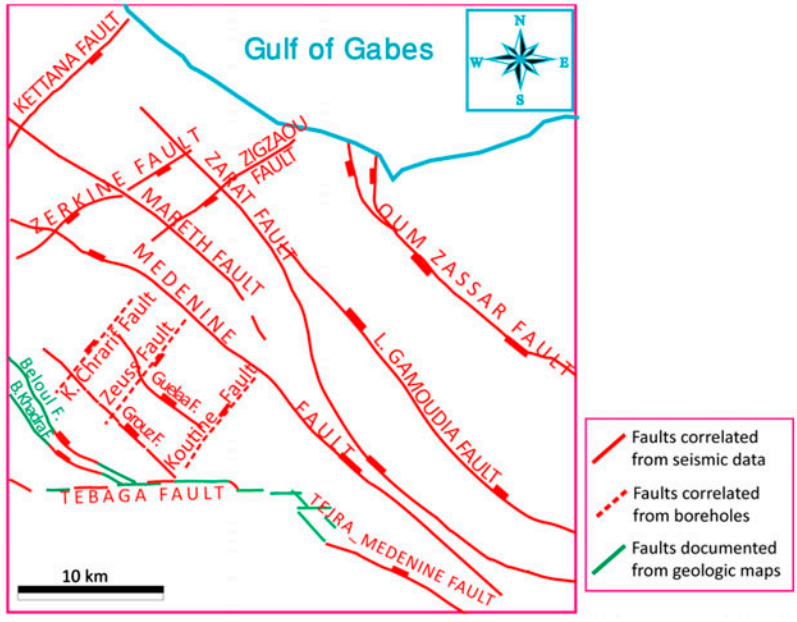

Fig. 3. Fault network correlated from seismic and geological data.

The weights are chosen so as to minimize the estimation error variance:

$$\sigma_{\kappa}^2 = Var[Z^*(x) - Z(x)] \quad (2)$$

under the constraint of unbiasedness of the estimator. These weights are obtained by solving the linear equations of the kriging system. Kriging requires the use and hence the estimation and modelling of a variogram function that describes the spatial variability of the random variable $Z(x)$:

$$\gamma(h) = \frac{1}{2} Var[Z(x) - Z(x+h)] \quad (3)$$

where h is the distance separating data $Z(x)$ and $Z(x+h)$.

2.3.2. Kriging with inequality constraints

To enhance the estimation of the target variable "depth", kriging with inequality constraint makes it possible to use the information obtained from wells not intercepting the target horizon.

Accordingly as shown on Fig. 4, kriging with inequality constraints can take into account "hard data" consisting of exact values: $Z(x_\alpha) = z_\alpha, \alpha = 1, \ldots, m$, and complementary "inequality data" $Z(x_\alpha) \in A_\alpha = [a_\alpha; -\infty[, \alpha = m+1, \ldots, n$, where the

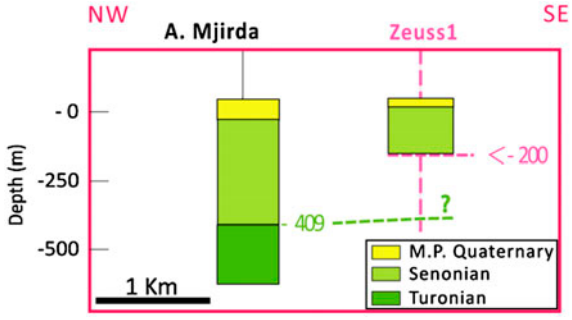

Fig. 4. Geological cross-section showing the available data for the Top Turonian reservoir:
exact data: borehole data corresponding to the geological interfaces: $Z(x)_{\text{A. Mjirda}} = -409$ m,
inequality data: information provided by the end of drilling: $Z(x)_{\text{Zeuss 1}} < -200$ m.

datum value z_α is only known to lie within an interval A_α.

The method is based on a two-step process.

First, inequality data have to be replaced by a new set of exact data consistent with the original exact points. The way to replace the intervals is to calculate the conditional expectation of the target variable at each inequality data location Z^{CE}_α. To calculate the conditional expectation, a Gibbs Sampler [10] technique is used to simulate, for each inequality, a given number of realizations of the target variable according to its variogram model and conditioned by the intervals and the exact data [8]. Then, the average value of the realizations at each inequality data point is calculated. These average values are an approximation to the conditional expectation.

The simulation of $Z^{CE}_\alpha, \alpha = m+1, \ldots, n$ conditionally on: $Z_\beta = z_\beta, 1 \le \beta \le m$ and $Z_\beta \in A_\beta, m+1 \le \beta \le n$ including $\beta = \alpha$ is implemented by repeating the following sequence:

(1) Assign a random value z_α within $A_\alpha = [a_\alpha; -\infty[$ for each site $x_\alpha, \alpha = m+1, \ldots, n$
(2) Select an index α_0 at random in the set of inequality data $\{\alpha = m+1, \ldots, n\}$.
(3) Ignore the value at this site and estimate it by kriging from the current values z_β at all other sites; also compute the corresponding kriging variance $\sigma^{*2}_{\alpha 0}$.
(4) Replace the value at this site by the kriged value plus a simulation of the error, conditionally on the inequality data at $x_{\alpha 0}$: the new $z_{\alpha 0} = Z^K_{\alpha 0} + \sigma^*_{\alpha 0}\, U$ where U is a standard normal random variable chosen so that $z_{\alpha 0}$ honours the inequality.
(5) Go back to 2, and loop many times.
(6) Calculate the conditional expectation at this site by averaging the set of simulations $z_{\alpha'} (\alpha = m+1, \ldots, n)$. The conditional expectation $Z^{CE}_{\alpha 0}$ is in fact the most probable value of the variable at the inequality data locations.

$$Z^{CE}_{\alpha 0} = E[Z(x) \backslash Z_\alpha \in A_{\alpha'} \forall \alpha] = \sum_\beta \lambda_\alpha E[Z_\beta \backslash Z_\alpha \in A_{\alpha'} \forall \alpha] \quad (4)$$

Then, the second step is to estimate the target variable using ordinary kriging with both the exact data and the conditional expectation values that replace the inequalities. It is also possible to consider the conditional variance σ^{*2}_α derived from the simulations (step 6) as a variance of measurement error. This has the advantage of giving less confidence to the conditional expectation values than to the exact data. However, it should be noted that, by doing that, the resulting variance may still be too optimistic; indeed, we do not account for the fact that the errors made when replacing inequalities by the conditional expectation are not independent.

3. Results

The results shown are for the estimation of the Turonian upper boundary. Remember that our case study is characterized by two main features that make the modelling task relatively difficult: (i) the spatial distribution of values is random, in that some observations are close to each other and some others are scattered. (ii) Geometric fault parameters compartmentalize the reservoir surface into subdomains with different data density. These two features are two major causes of uncertainties. An important contribution of geostatistics is the assessment of the uncertainty on unsampled values that usually helps to handle compartments with different data density and thus to choose the relevant kriging method.

A key step before prediction is the modelling of the spatial distribution of Turonian depth variable. The experimental variograms were calculated in two specific directions (Fig. 5): along the normal NW-SE faults, the major continuity direction; and across the faults that is along the SW-NE subsidence direction. This variogram shows an extremely high variability owing to the fact that it may include couples where x and $x+h$ are taken in two different compartments.

The directional variograms show an anisotropic behaviour: (i) A stationary structure expressed in the NW-SE direction. This locally stationary structure is

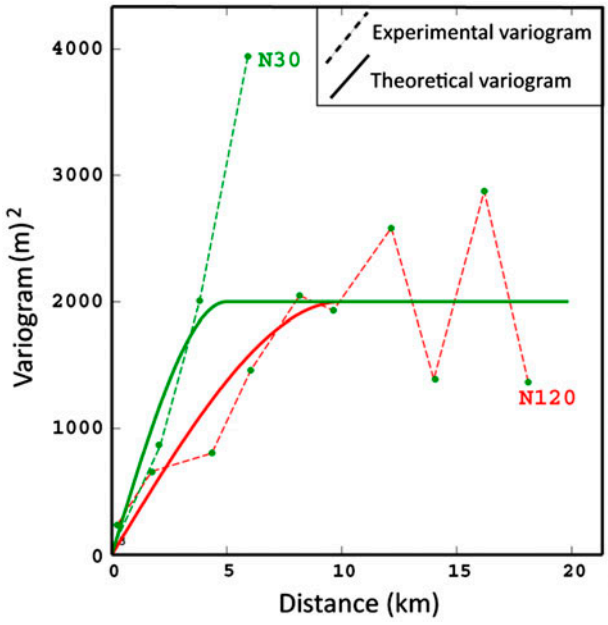

Fig. 5. Directional variograms of the Turonian Horizon. N30: NE-SW directional variogram, N120: NW-SE directional variogram.

related to the depth variability, at a small scale, within each compartment. (ii) A drift structure expressed in the NE-SW direction. The drift structure reflects the continuous increase in the depth within the overall down-tilted study area towards the NE direction.

For each target location, the neighbouring samples must be located within the considered compartment, between the fault boundaries. Therefore, the model parameters must be inferred from variogram values from only a few distance classes. Accordingly, the variogram has to be fitted on the basis of their behaviour towards small and medium distances, only the stationary behaviour is taken into account for depth interpolation. The variogram was fitted with an anisotropic stationary spherical structure with a range of 10,000 m along the NW-SE direction and 5,000 m along the NE-SW direction and a sill of 2000 m: $\gamma(h) = 2000\,spherical\,(10000_{N120}; 5000_{N30})$.

Ordinary kriging was applied using only exact data. Fig. 6(A) shows the kriged depth map of the top Turonian reservoir. It shows that ordinary kriging with local search neighbourhoods provides good results in the central compartment where the data density is high. This is confirmed by the low kriging variance values (Fig. 6(B)). On the contrary, in the NE compartments, ordinary kriging is inappropriate: there are inconsistencies resulting from two special properties of the estimating procedures: (i) the first concerns the neighbourhood information which has to be restricted inside the compartment and (ii) the second is the violation of the constraints at wells where the horizon has not been reached by the boreholes.

The method of kriging with inequality constraints makes it possible to take into account the constraint information obtained from wells which have not intercepted the target horizon. It makes the best use of the available data and thus increases neighbourhood information within each compartment. Fig. 7(A) shows the depth map of the top Turonian reservoir. It demonstrates that kriging, with a local search neighbourhood, is successful in all the compartments of the study area. In the NE compartments, the inequalities are now adequately taken into account in the modelling process. Associated kriging variance values are small even around the inequalities because, in the present case, most inequalities correspond to wells where the horizon has not been reached (depth $\geqslant$ certain value). Consequently, the probable value for these wells is close to the end of the borehole and the associated kriging variance is small. As discussed in the section above, obtained kriging variances might be

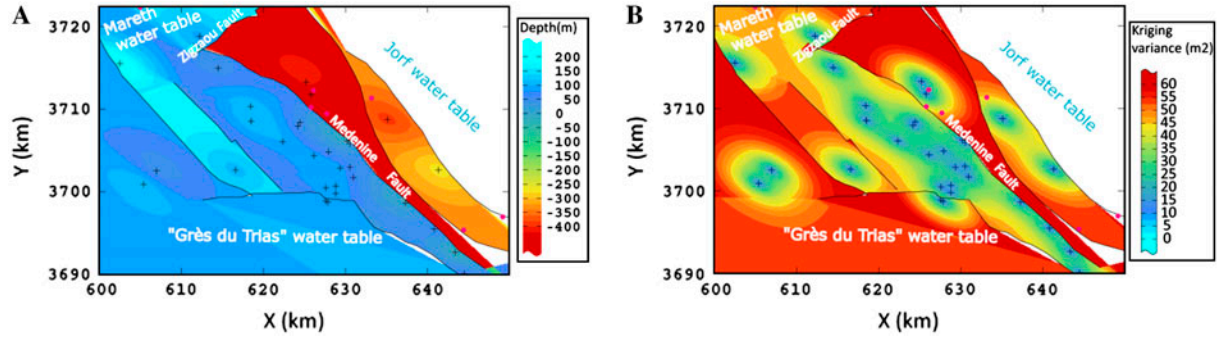

Fig. 6. (A): Depth map of the Top Turonian reservoir calculated by ordinary kriging. Location of exact data (black crosses +) and inequality data (pink circles ●). (B): Kriging variance map.

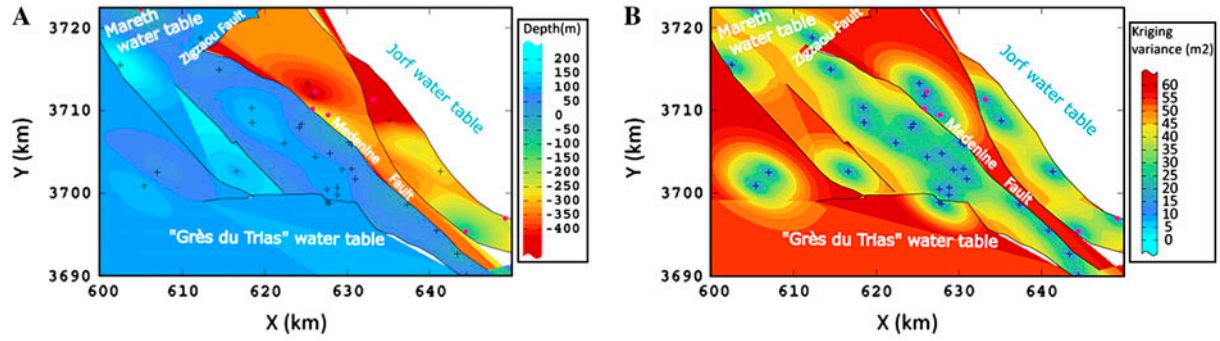

Fig. 7. (A): Depth map of the Top Turonian reservoir calculated by kriging with the inequalities method. Location of exact data (black crosses +) and inequality data (pink circles ●). B: Kriging variance map.

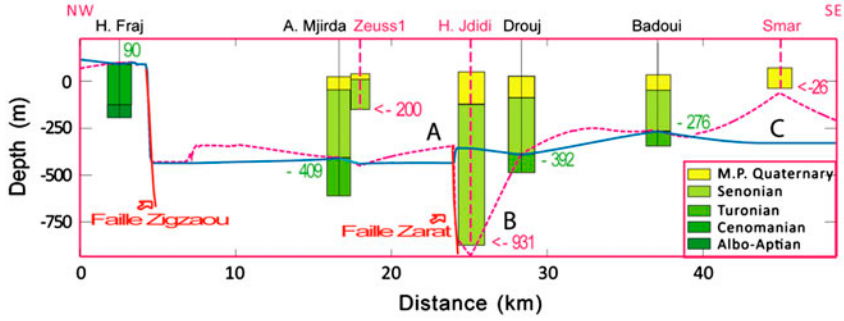

Fig. 8. Blue continuous line: Interpolated surface based on exact data only; Pink dashed line: Interpolated surface based on exact and inequalities. Boreholes designed in black are exact data and boreholes designed in pink are inequalities, the depth values are indicated for each borehole.

slightly underestimated as the correlation of errors is ignored.

Fig. 8 presents a NE-SW cross-section intersecting seven boreholes. Four of them are shown in black and represent the exact data and three boreholes are shown in pink and represent inequality data (the depth values of the Top Turonian reservoir are indicated for each borehole). This figure presents, as well, in blue continuous line the interpolated surface using ordinary kriging and in pink dashed line the interpolated surface with inequality constraints. Large differences between the two estimators arise particularly at A, B and C locations:

(1) In location A, ordinary kriging does not respect the dip direction of the Zarat Fault. In fact, the Zarat fault dips to the NE direction and not to the SW and this is a physically inconsistent result.
(2) In location B, ordinary kriging cannot directly handle the inequality constraints imposed by Henchir Jdidi well, this measurement is ignored and the surface is overestimated with a large kriging variance.
(3) In Location C, ordinary kriging violates the constraints at Smar well where the horizon has not been reached by the borehole, the surface is extrapolated with a large kriging variance.

Contrary to ordinary kriging, the constrained kriging method incorporates both the exact and the inequality data. It respects the dip direction at location A and improves the estimation in B and C. Also, kriging with inequality constraints provides a smaller kriging variance in areas only informed with inequalities (Fig. 6(A) and (B)).

4. Conclusions and perspectives

Characterizing aquifer systems in faulted settings with scarce data is a challenging task. The "Jeffara de Medenine" aquifer, in South-Eastern Tunisia, is a case in point. The complex geological setting required first a thorough review of the available data in order to build a detailed structural framework that constituted the fundamental part of the geometric modelling. Afterwards, it was shown how appropriate geostatistical modelling can provide suitable estimates for the target faulted surface. The applied kriging approach accurately integrated both exact

data and inequality constraints, improving predictions of each horizon.

To enhance the estimation of a given horizon, it might be possible to incorporate the correlation between successive horizons within a cokriging approach. Although classical, this method is complicated and requires further work in the present case as the relationships between the different horizons may vary from one geological compartment to another.

Improved procedures for estimating geologic interfaces make it possible to build geometric models that reflect as well as possible the geological reality, which results in a better assessment of water resources and subsequently a better management of the aquifer system.

Symbols

$Z(x_\alpha)$ — Regionalized variable (depth), m
$Z^*(x)$ — $Z(x)$ estimator, m
$\gamma(h)$ — A variogram function that describes the spatial variability of the regionalized variable $Z(x)$, m^2
λ_α — Kriging weights
σ_κ^2 — Kriging variance, m^2
Z_α^{CE} — Conditional expectation of $Z(x_\alpha)$, m
A_α — Inequality interval $A_\alpha = [a_\alpha; -\infty]$

References

[1] Geovariances, ISATIS 2012 technical references, 2012.
[2] G. Busson, Le Mésozoïque saharien 1re partie: l'extrême-Sud tunisien, Publications du Centre de Recherches sur les Zones Arides (CNRS) [Part 1: The extreme Southern Tunisia, Publications of the Research Centre on Arid Zones (CNRS)], Paris, série Géologie, 8, 1967, p. 194.
[3] B. Ben Baccar, Contribution à l'étude hydrogéologique de l'aquifère multicouche de Gabès Sud [Contribution to the hydrogeological study of multilayer aquifer South of Gabes], Doctoral thesis, University of Paris Sud, Orsay, 1982.
[4] A. Mammou, Caractéristiques et évaluation des ressources en eau du Sud Tunisien [Characteristics and evaluation of water resources in Southern Tunisia], PhD thesis, University of Paris-Sud, Orsay, 1990.
[5] H. Chihi, Fault system analysis of the Zeuss-Koutine aquifer (Southern Tunisia): New insights into reservoir modelling, Fifth international Symposium of IGCP 506 on: Marine and Non-Marine Jurassic Global Correlation and Major Geological Events, Hammamet, Tunisia, March 28–31, 2008.
[6] H. Chihi, M. Bedir, H. Belayouni, Variogram identification aided by a structural framework for improved geometric modeling of faulted reservoirs: Jeffara Basin, Southeastern Tunisia, Natural Resources Research 22(2) (2013) 139–161. doi: 10.1007/s11053-013-9201-0.
[7] S. Bouaziz, Geologic map of Medenine (1/100.000), 1990.
[8] J.P. Chilès, P. Definer, Geostatistics: Modelling Spatial Uncertainty, John Wiley & Sons, New York, 2012.
[9] G. Matheron, Pour une analyse krigeante des données régionalisées [For Kriging analysis of regionalized data], Technical Report N-732, Centre de Géostatistique [Centre for Geostatistics], Fontainebleau, France, 1982.
[10] S. Gemanand, D. Geman, Stochastic relaxation, Gibbs distribution and the Bayesian restoration of images, IEEE Trans. Pattern Anal. Mach. Intell. 6 (1984) 721–741.